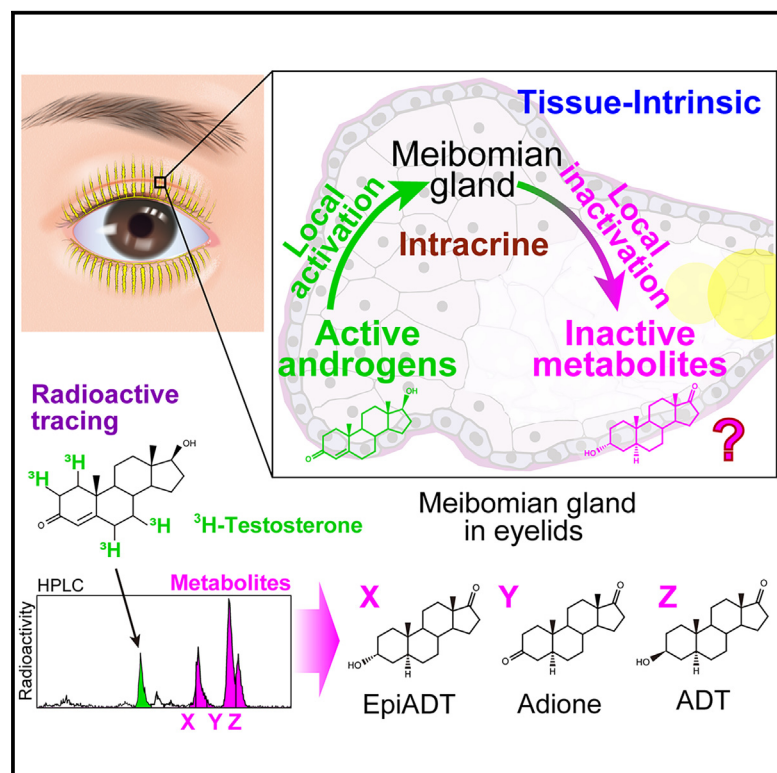


Identification of meibomian gland testosterone metabolites produced by tissue-intrinsic intracrine deactivation activity

Graphical abstract



Authors

Khanh Tien Nguyen Pham,
Takahito Miyake, Tomo Suzuki, ...,
Takeshi Nakajima, Emi Hasegawa,
Masao Doi

Correspondence

doimasao@pharm.kyoto-u.ac.jp

In brief

Biochemistry; Molecular Biology;
Physiology

Highlights

- Eyelid meibomian glands endogenously deactivate testosterone
- The meibomian gland testosterone metabolites are conserved between humans and mice
- There is no sex-related difference in meibomian testosterone metabolism
- Enzymes for testosterone production and deactivation are present in meibomian cells



Article

Identification of meibomian gland testosterone metabolites produced by tissue-intrinsic intracrine deactivation activity

Khanh Tien Nguyen Pham,¹ Takahito Miyake,¹ Tomo Suzuki,^{2,3} Shigeru Kinoshita,⁴ Yuki Hamada,¹ Hikari Uehara,¹ Mamiko Machida,⁵ Takeshi Nakajima,⁵ Emi Hasegawa,¹ and Masao Doi^{1,6,*}

¹Department of Systems Biology, Graduate School of Pharmaceutical Sciences, Kyoto University, Sakyo-ku, Kyoto 606-8501, Japan

²Department of Ophthalmology, Kyoto Prefectural University of Medicine, Kamigyō-ku, Kyoto 602-0841, Japan

³Department of Ophthalmology, Kyoto City Hospital, Nakagyō-ku, Kyoto 604-8845, Japan

⁴Department of Frontier Medical Science and Technology for Ophthalmology, Kyoto Prefectural University of Medicine, Kamigyō-ku, Kyoto 602-0841, Japan

⁵Senju Laboratory of Ocular Sciences, Senju Pharmaceutical Co., Ltd., Kobe 650-0047, Japan

⁶Lead contact

*Correspondence: doimasao@pharm.kyoto-u.ac.jp

<https://doi.org/10.1016/j.isci.2025.111808>

SUMMARY

Intracrinology—wherein hormones are synthesized in the organ where they exert their effect without release into circulation—has been described. However, molecular mechanisms of hormone deactivation within intracrine tissue are still largely unknown. The meibomian glands in the eyelids produce oil (meibum) to the ocular surface to prevent dehydration (dry eye). Androgens are generated inside this gland and are crucial for its tissue-homeostasis. However, there is no data showing the presence of androgens in meibum, implying local conversion/deactivation into unknown metabolites. Here, we performed radioactive tracer studies in combination with pharmacological enzyme inhibition, followed by targeted liquid chromatography-tandem mass spectrometry (LC-MS/MS) analysis, and found three androgen metabolites—androstanedione, androstosterone, and epiandrosterone—in mouse and human meibomian glands. Accounting for the enzymatic conversion, we show tissue-endogenous $3\alpha/3\beta$ -ketosteroid reductase expression. We therefore reinforce the idea that androgens are metabolically inactivated within the glands. These metabolite markers may help to assess meibomian local androgen activity using meibum.

INTRODUCTION

Canonically, hormones are produced by endocrine organs and delivered to distal target tissues. However, for steroids, the concept of “intracrinology,” whereby hormones are synthesized in the tissue where they exert their effect without release into circulation, has been described^{1–3} for a number of extra-gonadal tissues such as uterine endometrium^{4–6} and skin sebaceous gland^{7,8} as well as several cancerous tissues including those of the prostate,^{9,10} breast,^{11,12} and bone.¹³ Yet, the mechanisms by which active steroid hormones are degraded in intracrine tissues are still not fully understood. The degradation or deactivation of bioactive steroids is as crucial as the synthesis of new ones in determining the timing and location of their biological effects *in vivo*. Our study focuses on the degradation process of steroid hormones in the meibomian gland, a recently recognized intracrine tissue¹⁴ situated in the tarsal plate of the eyelids.

The meibomian glands are responsible for producing and secreting an oily substance called meibum. This meibum oil forms a crucial part of the tear film that covers the ocular surface. The primary function of meibum is to slow down the evaporation of the tear film, thereby preventing the eyes from drying out and

maintaining proper lubrication for optimal vision. Therefore, dysfunction of the meibomian glands leads to dry eye conditions and other ocular surface disorders; particularly, it is recognized that meibomian gland dysfunction is clinically the most common cause of evaporative dry eye disease.^{15–21}

Androgens are generated or activated inside the meibomian glands in both females and males, and these hormones are crucial to promote meibum production.¹⁵ The meibomian gland acinar cells express the androgen receptor (AR)^{22,23} and its activation causes upregulation of meibum production through a holocrine mechanism.^{14,15} Androgen deficiency—such as that caused by antiandrogen clinical treatment—has been reported to be associated with the development of meibomian gland dysfunction.^{24,25} Thus, evidence suggests that measuring androgen activity within the meibomian gland could be clinically relevant in understanding the etiology of meibomian gland dysfunction and its related dry eye symptoms.^{26,27} However, at present, there is no clinical biomarker to reflect local androgen activity in the meibomian gland.

At the molecular level, we previously demonstrated that the meibomian gland acinar cells express the type I 3β -hydroxysteroid dehydrogenase (type I 3β -HSD, or HSD3B1), which allows



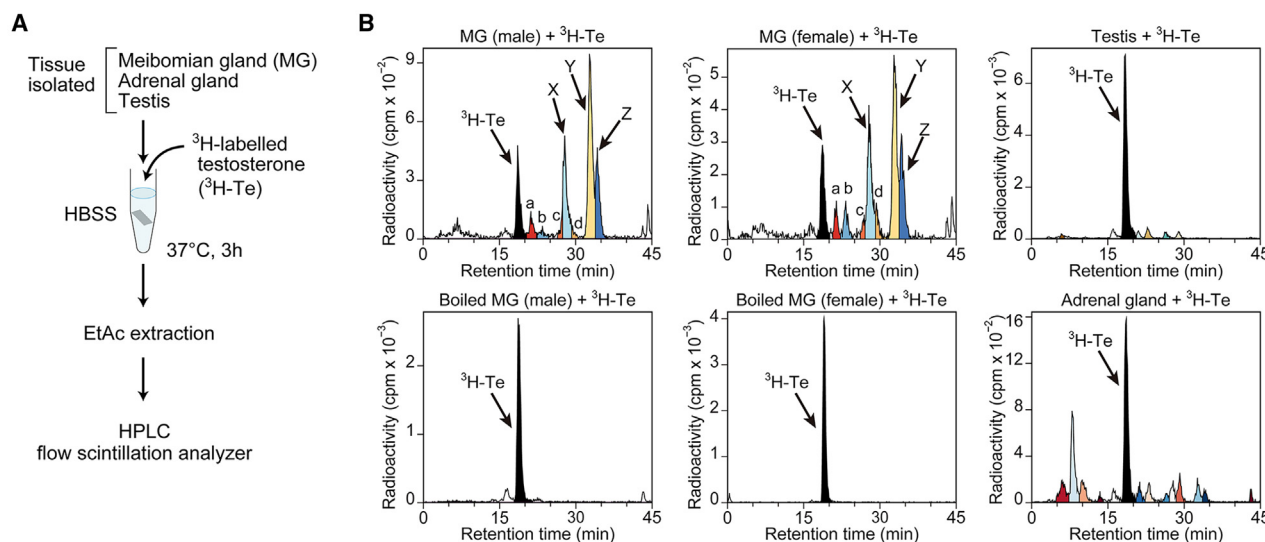


Figure 1. Tracing of tissue-endoogenous testosterone metabolism in the meibomian gland

(A) Schematic illustration of radioisotopic testosterone tracing. Freshly isolated mouse tissues were incubated *in vitro* with ^3H -labelled testosterone (^3H -Te) and its metabolites were detected using an HPLC-flow scintillation analyzer.

(B) Representative chromatograms showing metabolites of testosterone in the meibomian gland of male and female mice. Boiled male and female meibomian gland tissues serve as control. Metabolites in the adrenal gland and testis were analyzed in comparison. Peaks labeled as X, Y, Z, a, b, c, and d in the meibomian gland were analyzed in Figures 2 and 3.

on-site production of androgens (conversion of their precursor substrates to active androgens) in the meibomian gland.¹⁴ These locally activated hormones are believed to function only in the meibomian gland, because they are likely inactivated in the same tissue. This localized hormone action likely ensures that hormones exert their effects only in the tissue where they are produced. While part of the mechanism of androgen synthesis in the meibomian gland has been elucidated,^{14,28} the equally important process of hormonal inactivation remains less understood. Specifically, the molecular identity of androgen metabolites and the enzymes responsible for their inactivation are still unknown.

There are comprehensive lipidome studies characterizing the meibum in humans; however, none reported the existence of androgens, such as testosterone (Te), in human meibum samples tested.^{29–35} This absence may be due to the low levels of Te, possibly because it is inactivated into other metabolites. The current study, therefore, aimed to identify tissue-endoogenous Te metabolites in human and mouse meibomian gland. To this end, we first traced candidate Te metabolites in mice and then applied these findings to humans by analyzing human meibum metabolites.

RESULTS

Tracing testosterone metabolites

To gain insight into previously uncharacterized tissue-endoogenous metabolism or catabolism of testosterone within the meibomian gland, we initiated our study by performing radioisotopic tracer experiments using mouse tissues incubated with radioactive tritium-labeled testosterone (^3H -Te) (Figure 1A). Metabolites were separated by HPLC, followed by radioisotope measurement using an online-linked flow scintillation analyzer (see

STAR Methods). Freshly isolated mouse whole meibomian gland tissues, incubated *in vitro* with ^3H -Te, produced three dominant radioactive metabolites with retention times of 28 min (peak X), 33 min (peak Y), and 34 min (peak Z), with minor or trace amounts of radioactive products around 21 min (peak a), 23 min (b), 27 min (c), and 29 min (d), all of which were undetectable in boiled meibomian tissue (see Figure 1B). There was no obvious sex-related difference as revealed by similar radioactive products of ^3H -Te in the meibomian gland of female mice. In comparison, testosterone (^3H -Te) largely remained unconverted after incubation with the isolated testis or the adrenal gland. A different product peaking around 8 min was mainly observed in the adrenal gland (Figure 1B), indicating that the meibomian gland possesses a tissue-unique and potent metabolic activity against testosterone.

Effects of blocking 5α -reductase and aromatase on meibomian gland Te metabolites

To gain insights into the nature of meibomian gland Te metabolites, we first examined the influence of blocking 5α -reductase and aromatase on the appearance of each product (Figure 2A). We observed that all products except a (that is, X, Y, Z, b, c, and d) were profoundly reduced by the treatment of dutasteride, a 5α -reductase inhibitor (Figure 2B). The peak area ratios of X, Y, and Z were significantly decreased upon dutasteride treatment relative to those of vehicle control, with an accompanied significant increase of the peak area of a (Figure 2B). On the other hand, fadrozole, a specific inhibitor for aromatase, did not produce statistically significant effect on the appearance of metabolites (Figure 2B), indicating that the metabolites X, Y, Z, and others were raised through 5α -reductase, not aromatase, and that the metabolite a was produced at the expense of the inhibited 5α -reductase-mediated metabolism to X–Z.

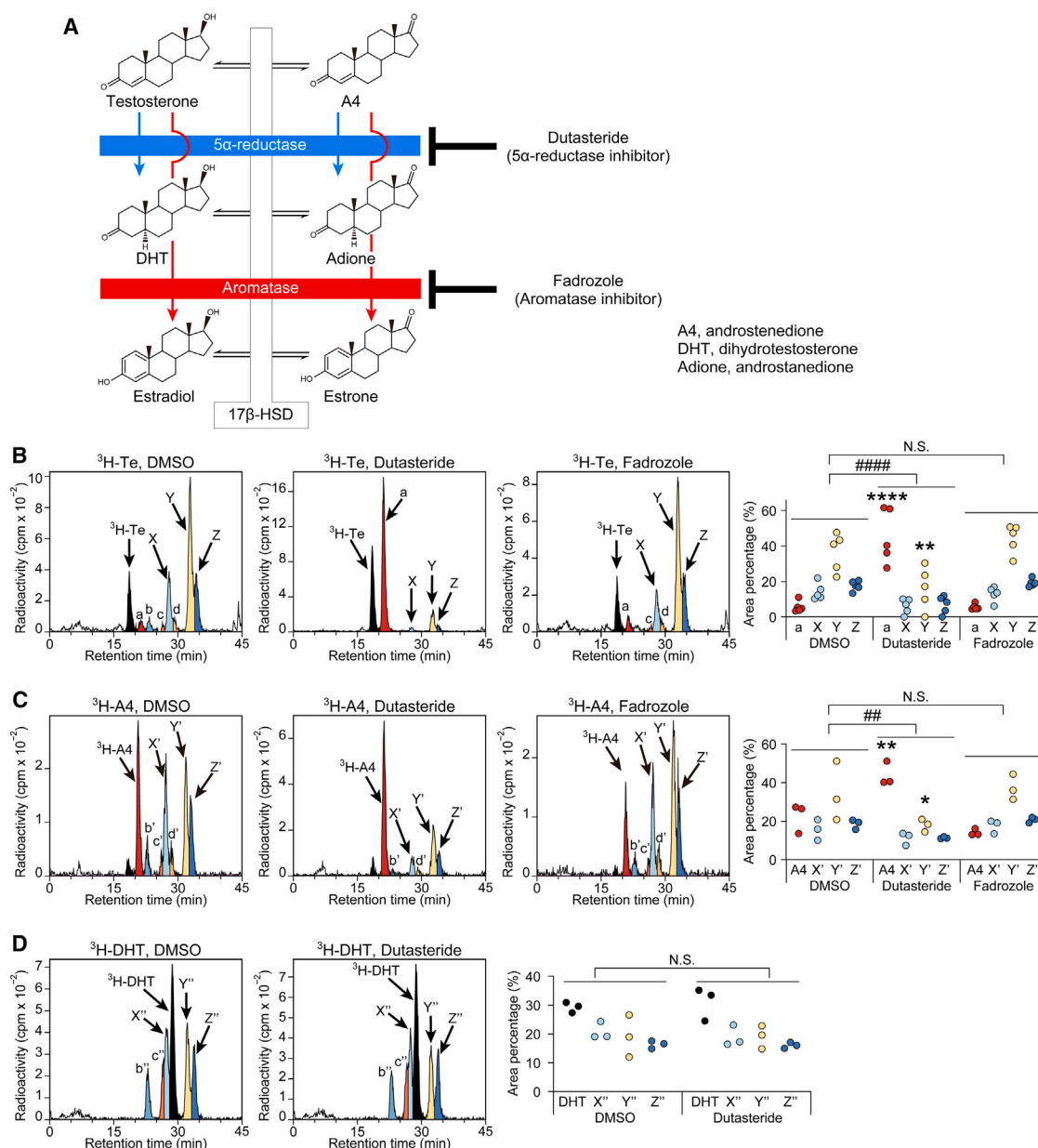


Figure 2. Effects of pharmacological inhibition of 5 α -reductase by dutasteride and aromatase by fadrozole on the testosterone metabolism in the meibomian gland

(A) Potential metabolic pathway of Te and A4 via 5 α -reductase (blue) and aromatase (red).

(B) Example chromatograms and peak-area ratio of $^3\text{H-Te}$ metabolites in the meibomian gland incubated with dutasteride, fadrozole or vehicle (0.5% DMSO) ($n = 5$ for each condition).

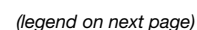
(C) Example chromatograms and peak-area ratio of $^3\text{H-A4}$ metabolites in the meibomian gland incubated with dutasteride, fadrozole or vehicle (0.5% DMSO) ($n = 3$ for each condition).

(D) Example chromatograms and peak-area ratio of $^3\text{H-DHT}$ metabolites in the meibomian gland treated with dutasteride or vehicle (0.5% DMSO) ($n = 3$ for each). Data in (B), (C) and (D) were analyzed using two-way analysis of variance (ANOVA) followed by Bonferroni's post hoc test. ANOVA interaction: ## $p < 0.01$, ### $p < 0.0001$, N.S., not significant. * $p < 0.05$, ** $p < 0.01$, **** $p < 0.0001$ versus each DMSO control. A4, androstenedione; DHT, 5 α -dihydrotestosterone.

Androstenedione and 5 α -dihydrotestosterone are not metabolites X, Y, and Z

Next, the RI tracer experiments were performed using different substrates (Figures 2C and 2D). Androstenedione (A4) is a potential Te metabolite that could accumulate upon the blockade of

5 α -reductase (see Figure 2A). We thus assumed that the product a might be A4. Consistently, ^3H -labeled A4 ($^3\text{H-A4}$) not only had the same retention time as the metabolite a in the chromatogram but also produced three dominant metabolites, most likely X, Y, and Z, in a manner that depended on 5 α -reductase activity (Figure 2C).



We also speculated that 5 α -dihydrotestosterone (DHT) might be included among the major metabolites X–Z. However, this was not the case. ³H-labeled DHT eluted at a similar elution time as d and was converted into radioactive products resembling X, Y, Z, b, and c (but not a) (Figure 2D); These conversions were not affected by dutasteride treatment (Figure 2D), consistent with DHT being already a 5 α -reduced product of Te (see a metabolic pathway, Figure 2A). These data suggest that the three major metabolites, X, Y, and Z, are likely 5 α -reduced testosterone metabolites or their derivatives, distinct from DHT.

Mass spectrometric identification of meibomian gland Te metabolites

To characterize the identity of meibomian gland Te metabolites, we next utilized targeted liquid chromatography-tandem mass spectrometry (LC-MS/MS) approach (Figure 3). To this end, we searched for the presence of androstenedione (adione), androsterone (ADT), epiandrosterone (epiADT), DHT, 5 α -androstane-3 α ,17 β -diol (3 α -diol), and 5 α -androstane-3 β ,17 β -diol (3 β -diol), all of which are potential 5 α -reduced Te metabolites, in addition to A4—the 17-oxidized metabolite (metabolite a) tested in Figure 2C. Non-radioactive Te was incubated *in vitro* with isolated meibomian tissues, and metabolites were identified by comparing the mass spectra and retention times with those of the authentic standards (Figures S1 and 3A). In the uppermost chromatogram in Figure 3A, radioactive ³H-Te metabolites were separated using the same LC conditions as the mass spectrometry to facilitate comparison of the metabolites' retention times. With these conditions, we obtained LC-MS/MS chromatograms consistent with the idea of the Te metabolites X, Y, Z, a, b, and c being epiADT, adione, ADT, A4, 3 β -diol, and 3 α -diol, respectively (Figure 3A). All these metabolites were not produced in boiled meibomian gland (Figure 3A, red chromatograms). Moreover, in dutasteride-treated meibomian glands (Figure 3B), the production of epiADT (X), adione (Y), and ADT (Z) was suppressed, while A4 (a) and Te accumulated, compatible with the data in Figure 2B, which supports the identification of X, Y, and Z as epiADT, adione, and ADT, respectively. Our data therefore suggest that in the meibomian gland, the 5 α -reduced A4 metabolite, which is adione (Y, see a schematic in Figure 3C), is converted into two distinct enantiomeric metabolites, ADT (Z) or epiADT (X), through the enzymatic reaction via the 3 α -ketosteroid reductase (3 α -KSR) or 3 β -ketosteroid reductase (3 β -KSR), respectively (Figure 3C).

Detection of Te metabolites in human meibum

Based on our initial motivation, we finally inquired whether the identified three major Te metabolites can be found in meibum samples taken from human eyelids (Figure 4). Meibum samples were obtained from healthy volunteers as described in STAR

Methods (see also Figure 4A). To enhance the MS/MS sensitivity, we employed a quaternary aminoxy (QAO) reagent to derivatize the carbonyl functional group of Te, epiADT, adione, and ADT (see Figure 4B, left). Te was undetectable or below the lower limit of quantitation (LOQ) in almost all human meibum samples tested (Figure 4C; see also Table S1). On the other hand, adione, ADT, and epiADT (the three major mouse Te metabolites) were all readily detectable with an average concentration normalized by total cholesterol of 0.30 ± 0.02 (SEM) fmol/nmol for adione, 0.05 ± 0.005 fmol/nmol for ADT, and 0.03 ± 0.002 fmol/nmol for epiADT. There was no sex-related difference in the amount of metabolites (mean \pm SEM, fmol/nmol, for adione, male, 0.32 ± 0.02 , female, 0.27 ± 0.04 ; ADT, male, 0.05 ± 0.005 , female, 0.05 ± 0.01 ; epiADT, male, 0.03 ± 0.003 , and female, 0.02 ± 0.003) (Figure 4C), reminiscent of the similarity between male and female Te metabolite profiles traced in mice (Figure 1B).

As shown in Figure 4D, existence of ADT and epiADT in human meibum samples was further corroborated by immunostaining of the corresponding enzyme; We used a specific antibody to AKR1C3 and AKR1C4 (anti-AKR1C3/4) because the enzymes encoded by human *AKR1C3* and *AKR1C4* are reported to exhibit 3 α /3 β -KSR activity *in vitro*^{36,37} and expression surveys using accessible transcriptome datasets for human meibomian gland tissue and cells point to the presence of these enzymes among the other AKR1C subtypes at the mRNA level.^{38,39} We also used a specific antibody to HSD3B1, which is the enzyme essential for producing androgen⁴⁰ and has been demonstrated to be present in the meibomian gland cells of both men and women,¹⁴ for comparison.

Immunohistochemistry (Figure 4D) revealed strong anti-AKR1C3/4 immunoreactivities within the meibomian gland acinar cells, but not in duct/ductule cells or adjacent connective tissues. Anatomically, each single meibomian gland is composed of multiple acini connected via short ductules to a long central duct that extends to the orifice at the eyelid margin^{17,41}; anti-AKR1C3/4 immunoreactivities were detected in nearly all acini and broadly distributed within each of them (Figure 4D). A similar staining pattern was also observed using a different antibody (see Figure S2). Moreover, no obvious difference was observed between male (Figure 4D, left) and female (Figure 4D, right) eyelids, consistent with the detection of similar metabolites in both sexes.

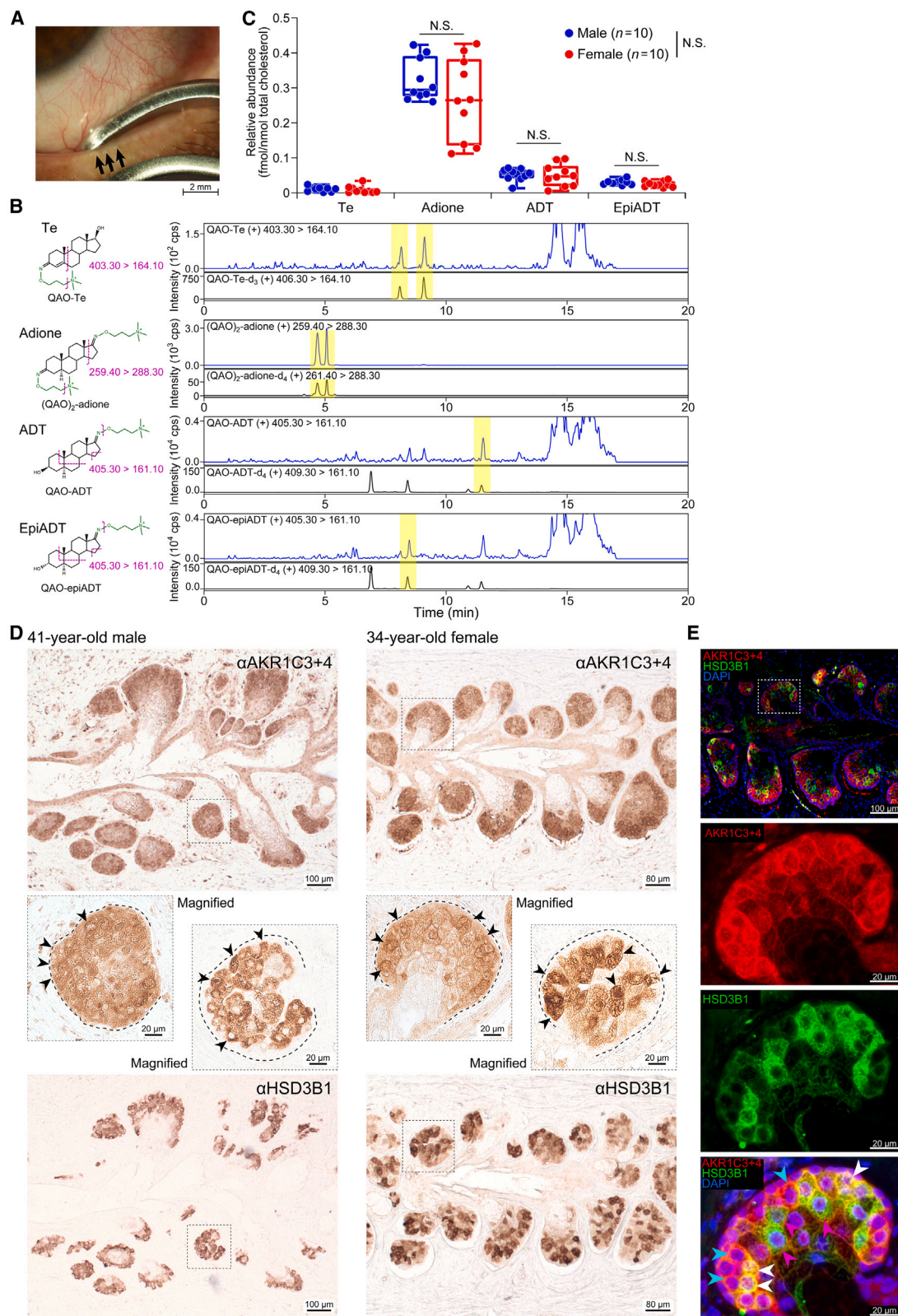
The expression of HSD3B1, an androgen-producing enzyme, was distributed in acini but in a mosaic distribution pattern,¹⁴ resulting in the observation that nearly all HSD3B1-immunopositive cells (green) are also immunopositive for AKR1C3/4 (red), but not vice versa (Figure 4E, dual-label immunofluorescence for HSD3B1 and AKR1C3/4) (see also serial flip-flop tissue sections for HSD3B1 and AKR1C3/4, Figure 4D). It is likely that Te in the meibomian gland is metabolized inside as well as outside of the HSD3B1-positive cells by AKR1C3/4.

Figure 3. Mass spectrometric characterization of testosterone metabolites produced by the meibomian gland

(A) LC-MS/MS MRM total ion chromatograms of testosterone (Te) and potential testosterone metabolites, androstenedione (A4), epiandrosterone (epiADT), androstenedione (adione), androsterone (ADT), 5 α -androstane-3 β ,17 β -diol (3 β -diol) and 5 α -androstane-3 α ,17 β -diol (3 α -diol), of testosterone (non-radioactive)-treated meibomian gland (blue) and those with boiled meibomian gland (red). For comparison, RI chromatography was performed in parallel using the same LC method (top). Authentic standards serve to verify the retention time of metabolites (black). b, 3 β -diol; c, 3 α -diol; d, not determined.

(B) LC-MS/MS chromatograms of Te, A4, epiADT, adione and ADT of testosterone-treated meibomian gland with or without dutasteride application.

(C) Proposed testosterone metabolic pathway in the meibomian gland.



(legend on next page)

DISCUSSION

The current study was conducted to approach the identity of previously uncharacterized Te metabolite-species contained in the human meibomian gland's secretion. Not surprisingly, Te itself was not detected at a quantifiable concentration in human meibum samples tested.^{29–35} To approach the unknown metabolites, we took advantage of the hypothetical resemblance of mouse and human meibomian gland and traced the tissue-endogenous Te metabolism using the mouse meibomian gland tissue, which eventually led to identifying three Te metabolites, adione (androstenedione), epiADT (epiandrosterone), and ADT (androsterone) in human and mouse meibomian gland. No obvious sex-related difference was observed. These results support the notion that humans and mice exhibit similar tissue-endogenous androgen inactivation profiles in the meibomian gland (see Figure S3, a schematic summary of our findings).

Intracrine activity does not solely refer to the activity of hormone production *in situ* but it also denotes the activity of hormone inactivation inside the tissue where the hormone is produced and acts.^{1–13,42–46} Previously, we elaborated on the aspect of hormone production by showing the presence of 3 β -HSD enzyme responsible for the local androgen production in the meibomian gland¹⁴; however, the mechanism of hormone inactivation limb remains poorly understood. In the present study, we identified detectable amounts of three specific Te metabolites—epiADT, ADT, and adione—in human meibum samples. We also found that human meibomian gland acinar cells strongly express 3 α /3 β -KSR (AKR1C3/4), which aligns with the detection of epiADT and ADT. This enzyme catalyzes 3-ketosteroid reduction to inactivate androgens.³⁷ Of interest, the expression of 3 α /3 β -KSR (AKR1C3/4) was more broadly distributed than that of 3 β -HSD. This spatial relationship between 3 β -HSD (androgen-activating enzyme) and 3 α /3 β -KSR (androgen-inactivating enzyme) supports the concept of robust testosterone metabolism involving both 3 β -HSD-positive and negative cells (Figure S3). The large inactivation area surrounding the activation site likely explains the loss of detectable levels of Te during meibum secretion. In addition, the time that this secretion (holocrine) takes reaches as long as ~9 days, as reported in rats,⁴⁷ providing an additional reason for undetectable levels of Te in the meibum. This enzymatically robust deactivation system may also apply to other tissues; in skins, 3 α /3 β -KSR is reported to broadly distribute in epidermis,⁴⁸ while 3 β -HSD is confined to the sebaceous gland.⁴⁹ In breast and

prostate cancers, the expression of deactivation enzymes (such as estrogen sulfotransferase and glucuronosyltransferase) is negatively correlated with tumor progression and malignancy.^{50,51} These findings align with the principle of intracrinology, wherein hormones are inactivated within the same tissue where they are synthesized, thereby limiting the influence of bioactive hormones to the local region in which they are produced,^{1–13,42–46} and potential dysregulation of this system may lead to pathological conditions.

A more precise explanation may be necessary for clarifying why the meibomian Te metabolite species remained unidentified till our study. Indeed, despite comprehensive lipidome studies conducted for human meibomian gland excreta (meibum), adione, ADT, epiADT have so far escaped identification.^{29–35} This is likely largely due to the scant presence of Te metabolites, which are the catabolites of biological hormones, in the meibum, compared to other lipid constituents: cholesteryl esters (68% w/w), wax esters (25%), triacyl glycerol (5%), O-acyl- ω -hydroxy fatty acids (OAHFA) (4%), which are substantially more abundant than adione (0.3 fmol/nmol total cholesterol), ADT (0.05 fmol/nmol) and epiADT (0.03 fmol/nmol) (Figure 4C). Moreover, steroids are structurally similar compounds and also suffer from poor ionization efficiency in MS/MS analysis; thus targeted MS/MS approach with improved sensitivity is required. As such, in this study, we carried out radioactive tracer experiments in combination with pharmacological enzyme inhibition and thereby selected the potential Te metabolites for targeted LC-MS/MS analysis. Moreover, in order to detect trace concentrations of endogenous steroid hormone metabolites, we enhanced the MS/MS sensitivity by introducing an ionizable moiety (QAO) to the ketone group of each target metabolites. Employing the methodologies described above enabled detection of natural steroid hormone metabolites contained in human meibum.

A potential clinical application of our findings may include assessment of local androgen activity in the meibomian gland by quantifying androgen metabolites in meibum. Previous studies demonstrate that the human meibomian gland function is strongly influenced by sex steroid hormones, particularly androgens (see study by Bron et al.¹⁵ and references therein). In both females and males, androgens promote the synthesis and secretion of meibum lipids and suppress the expression of genes related to keratinization. Conversely, androgen deficiency—such as that seen in aging, Sjögren's syndrome, antiandrogen treatment, or complete androgen insensitivity syndrome—is associated with meibomian gland dysfunction, altered meibum

Figure 4. Human meibum testosterone metabolites and corresponding enzyme expression in the meibomian gland

(A) Meibum collection.

(B) Representative LC-MS/MS chromatograms showing QAO-derivatized Te, adione, ADT, and epiADT in human meibum specimen with chemical structure of each QAO-derivative shown on the left.

(C) Relative concentration of Te, adione, ADT, and epiADT in meibum specimen from men and women. For the boxplots, the center line indicates medians, the box boundaries mark the 25th and 75th percentiles, and the whiskers indicate minima and maxima. $n = 10$ per gender.

(D and E) 3 α /3 β -KSR expression in human meibomian gland. (D) Anti-AKR1C3+AKR1C4 (for human 3 β -KSR and 3 α -KSR) and anti-HSD3B1 immunohistochemistry using a pair of flip-flopped mirror image serial section from 41-year-old male and 34-year-old female eyelid specimen. The dotted boxes indicate the region of magnified view. Representative AKR1C3/4-immunopositive cells and HSD3B1-immunopositive cells are pointed by arrowheads. (E) Double-label immunofluorescence of AKR1C3+4 (red) and HSD3B1 (green). The dotted box, the region of magnified view. White arrowheads, AKR1C3+4- and HSD3B1-double positive cells. Blue arrowheads, AKR1C3+4-positive and HSD3B1-negative cells. Pink arrow heads, HSD3B1-dominant cells. Specimen, 34-year-old female meibomian gland.

Data in (C) was analyzed using two-way ANOVA followed by Bonferroni's post hoc test. N.S., not significant.

lipid profiles, and decreased tear film stability.^{17,25,52,53} Accumulating data thus suggest the potential clinical importance of measuring local androgen activity to understand the etiology of meibomian gland dysfunction and to develop therapies for ameliorating this condition.^{3,16} In this context, we identified specific androgen metabolites in meibum. Meibum is clinically accessible lipid excreta from the meibomian gland. These metabolite markers may help to provide a unique opportunity to assessing local-tissue androgen activity. Although further studies are required, these metabolites may contribute as a clinical surrogate endpoint for assessing meibomian gland dysfunction or dry eye, particularly in the context of drug discovery and development for these unmet medical conditions.^{54,55}

Collectively, in the present study, we have elucidated the molecular identity of the tissue-endogenous androgen metabolism in the meibomian gland. The deactivation of active steroid hormones is equally important as their *de novo* synthesis in determining the time and space of their actions. Our studies contribute to understanding the intracrine system of the meibomian gland, encompassing both the generation and deactivation of local steroid hormones. Our methods used in this study and results/findings may pave the way to understand the local steroid-hormone system reported in other intracrine tissues.

Limitations of the study

The potential of the identified metabolites, adione, ADT, and epi-ADT, for assessing local androgen activity in patients with different meibomian gland disorders or symptoms remains to be explored. Our currently available data are only confined to healthy subjects with no eye-related diseases. Although these metabolites have the potential to serve as a clinical surrogate endpoint in the evaluation of meibomian gland dysfunction or dry eye conditions, further research is still required.

RESOURCE AVAILABILITY

Lead contact

Further information and requests for resources should be directed to and will be fulfilled by the lead contact, Masao Doi (doimasao@pharm.kyoto-u.ac.jp).

Materials availability

This study did not generate new unique reagents.

Data and code availability

- All data reported in this paper will be shared by the [lead contact](#) upon request.
- This paper does not report original code.
- Any additional information required to reanalyze the data reported in this paper is available from the [lead contact](#) upon request.

ACKNOWLEDGMENTS

We thank Ryosuke Ochiai, Tsubasa Ibushi, and Tomoyo Yoshioka in Shimadzu Techno-Research for their expert assistance in LC-MS/MS studies. This work was supported in part by research grants from the Ministry of Education, Culture, Sports, Science and Technology of Japan (22H04987, 24H02306, 22K09771, and 24K02178), the Cyclic Innovation for Clinical Empowerment of the Japan Agency for Medical Research and Development (JP22pc0101069), Astellas Foundation for Research on Metabolic Disorders, SRF, Ono Medical Research Foundation, and Japan Endocrine Society Grant

for Promising Investigator. K.T.N.P. is supported by a Japan Science and Technology Agency SPRING fellowship.

AUTHOR CONTRIBUTIONS

M.D. conceived the project; M.D. and K.T.N.P. designed the research with T.S. and S.K.; K.T.N.P. performed experiments in collaboration with T.M., Y.H., H.U., M.M., T.N., and E.H.; T.S. and S.K. sampled human meibum samples; M.D., K.T.N.P., and T.M. wrote the paper with input from all authors.

DECLARATION OF INTERESTS

M.D., T.S., and S.K. received a research grant from Senju Pharmaceutical Co., Ltd. M.M. and T.N. are employed by Senju Pharmaceutical Co., Ltd.

STAR★METHODS

Detailed methods are provided in the online version of this paper and include the following:

- [KEY RESOURCES TABLE](#)
- [EXPERIMENTAL MODEL AND STUDY PARTICIPANT DETAILS](#)
 - Animals
 - Human participants
 - Human eyelid specimens
- [METHOD DETAILS](#)
 - Testosterone radioactive tracing
 - Testosterone tracing by LC-MS/MS
 - LC-MS/MS for human meibum profiling
 - Immunohistochemistry and immunofluorescence staining
- [QUANTIFICATION AND STATISTICAL ANALYSIS](#)

SUPPLEMENTAL INFORMATION

Supplemental information can be found online at <https://doi.org/10.1016/j.isci.2025.111808>.

Received: August 18, 2024

Revised: November 3, 2024

Accepted: January 10, 2025

Published: January 27, 2025

REFERENCES

1. Labrie, F. (1991). Intracrinology. *Mol. Cell. Endocrinol.* 78, C113–C118. [https://doi.org/10.1016/0303-7207\(91\)90116-a](https://doi.org/10.1016/0303-7207(91)90116-a).
2. Labrie, F., Martel, C., Bélanger, A., and Pelletier, G. (2017). Androgens in women are essentially made from DHEA in each peripheral tissue according to intracrinology. *J. Steroid Biochem. Mol. Biol.* 168, 9–18. <https://doi.org/10.1016/j.jsbmb.2016.12.007>.
3. Schiffer, L., Arit, W., and Störbeck, K.H. (2018). Intracrine androgen biosynthesis, metabolism and action revisited. *Mol. Cell. Endocrinol.* 465, 4–26. <https://doi.org/10.1016/j.mce.2017.08.016>.
4. Huhtinen, K., Desai, R., Stähle, M., Salminen, A., Handelsman, D.J., Perheentupa, A., and Poutanen, M. (2012). Endometrial and endometriot concentrations of estrone and estradiol are determined by local metabolism rather than circulating levels. *J. Clin. Endocrinol. Metab.* 97, 4228–4235. <https://doi.org/10.1210/jc.2012-1154>.
5. Gibson, D.A., McInnes, K.J., Critchley, H.O.D., and Saunders, P.T.K. (2013). Endometrial Intracrinology—generation of an estrogen-dominated microenvironment in the secretory phase of women. *J. Clin. Endocrinol. Metab.* 98, E1802–E1806. <https://doi.org/10.1210/jc.2013-2140>.
6. Gibson, D.A., Simitsidellis, I., Cousins, F.L., Critchley, H.O.D., and Saunders, P.T.K. (2016). Intracrine Androgens Enhance Decidualization and Modulate Expression of Human Endometrial Receptivity Genes. *Sci. Rep.* 6, 19970. <https://doi.org/10.1038/srep19970>.

7. Azmahani, A., Nakamura, Y., Felizola, S.J., Ozawa, Y., Ise, K., Inoue, T., McNamara, K.M., Doi, M., Okamura, H., Zouboulis, C.C., et al. (2014). Steroidogenic enzymes, their related transcription factors and nuclear receptors in human sebaceous glands under normal and pathological conditions. *J. Steroid Biochem. Mol. Biol.* 144, 268–279. <https://doi.org/10.1016/j.jsbmb.2014.07.010>.
8. Labrie, F., Luu-The, V., Labrie, C., Pelletier, G., and El-Alfy, M. (2000). Intracrinology and the skin. *Horm. Res.* 54, 218–229. <https://doi.org/10.1159/000053264>.
9. Locke, J.A., Guns, E.S., Lubik, A.A., Adomat, H.H., Hendy, S.C., Wood, C.A., Ettinger, S.L., Gleave, M.E., and Nelson, C.C. (2008). Androgen levels increase by intratumoral de novo steroidogenesis during progression of castration-resistant prostate cancer. *Cancer Res.* 68, 6407–6415. <https://doi.org/10.1158/0008-5472.CAN-07-5997>.
10. Montgomery, R.B., Mostaghel, E.A., Vessella, R., Hess, D.L., Kalhorn, T.F., Higano, C.S., True, L.D., and Nelson, P.S. (2008). Maintenance of intratumoral androgens in metastatic prostate cancer: a mechanism for castration-resistant tumor growth. *Cancer Res.* 68, 4447–4454. <https://doi.org/10.1158/0008-5472.CAN-08-0249>.
11. Santner, S.J., Feil, P.D., and Santen, R.J. (1984). In situ estrogen production via the estrone sulfatase pathway in breast tumors: relative importance versus the aromatase pathway. *J. Clin. Endocrinol. Metab.* 59, 29–33. <https://doi.org/10.1210/jcem-59-1-29>.
12. Labrie, F., Luu-The, V., Labrie, C., Bélanger, A., Simard, J., Lin, S.X., and Pelletier, G. (2003). Endocrine and intracrine sources of androgens in women: inhibition of breast cancer and other roles of androgens and their precursor dehydroepiandrosterone. *Endocr. Rev.* 24, 152–182. <https://doi.org/10.1210/er.2001-0031>.
13. Sandor, L.F., Huh, J.B., Benko, P., Hiraga, T., Poliska, S., Dobo-Nagy, C., Simpson, J.P., Homer, N.Z.M., Mahata, B., and Gyor, D.S. (2024). De novo steroidogenesis in tumor cells drives bone metastasis and osteoclastogenesis. *Cell Rep.* 43, 113936. <https://doi.org/10.1016/j.celrep.2024.113936>.
14. Sasaki, L., Hamada, Y., Yarimizu, D., Suzuki, T., Nakamura, H., Shimada, A., Pham, K.T.N., Shao, X., Yamamura, K., Inatomi, T., et al. (2022). Intracrine activity involving NAD-dependent circadian steroidogenic activity governs age-associated meibomian gland dysfunction. *Nat. Aging* 2, 105–114. <https://doi.org/10.1038/s43587-021-00167-8>.
15. Bron, A.J., de Paiva, C.S., Chauhan, S.K., Bonini, S., Gabison, E.E., Jain, S., Knop, E., Markoulli, M., Ogawa, Y., Perez, V., et al. (2017). TFOS DEWS II pathophysiology report. *Ocul. Surf.* 15, 438–510. <https://doi.org/10.1016/j.jtos.2017.05.011>.
16. Moreno, I., Verma, S., Gesteira, T.F., and Coulson-Thomas, V.J. (2023). Recent advances in age-related meibomian gland dysfunction (ARMGD). *Ocul. Surf.* 30, 298–306. <https://doi.org/10.1016/j.jtos.2023.11.003>.
17. Knop, E., Knop, N., Millar, T., Obata, H., and Sullivan, D.A. (2011). The international workshop on meibomian gland dysfunction: report of the subcommittee on anatomy, physiology, and pathophysiology of the meibomian gland. *Invest. Ophthalmol. Vis. Sci.* 52, 1938–1978. <https://doi.org/10.1167/iovs.10-6997c>.
18. Suzuki, T., Teramukai, S., and Kinoshita, S. (2015). Meibomian glands and ocular surface inflammation. *Ocul. Surf.* 13, 133–149. <https://doi.org/10.1016/j.jtos.2014.12.002>.
19. Sullivan, D.A., Rocha, E.M., Aragona, P., Clayton, J.A., Ding, J., Golebiowski, B., Hampel, U., McDermott, A.M., Schaumberg, D.A., Srinivasan, S., et al. (2017). TFOS DEWS II Sex, Gender, and Hormones Report. *Ocul. Surf.* 15, 284–333. <https://doi.org/10.1016/j.jtos.2017.04.001>.
20. Amano, S. (2018). Meibomian Gland Dysfunction: Recent Progress Worldwide and in Japan. *Invest. Ophthalmol. Vis. Sci.* 59, DES87–DES93. <https://doi.org/10.1167/iovs.17-23553>.
21. Tsubota, K., Yokoi, N., Watanabe, H., Dogru, M., Kojima, T., Yamada, M., Kinoshita, S., Kim, H.M., Tchah, H.W., Hyon, J.Y., et al. (2020). A New Perspective on Dry Eye Classification: Proposal by the Asia Dry Eye Society. *Eye Contact Lens* 46, S2–S13. <https://doi.org/10.1097/ICL.0000000000000643>.
22. Sullivan, D.A., Sullivan, B.D., Ullman, M.D., Rocha, E.M., Krenzer, K.L., Cermak, J.M., Toda, I., Doane, M.G., Evans, J.E., and Wickham, L.A. (2000). Androgen influence on the meibomian gland. *Invest. Ophthalmol. Vis. Sci.* 41, 3732–3742.
23. Rocha, E.M., Wickham, L.A., da Silveira, L.A., Krenzer, K.L., Yu, F.S., Toda, I., Sullivan, B.D., and Sullivan, D.A. (2000). Identification of androgen receptor protein and 5alpha-reductase mRNA in human ocular tissues. *Br. J. Ophthalmol.* 84, 76–84. <https://doi.org/10.1136/bjo.84.1.76>.
24. Sullivan, B.D., Evans, J.E., Krenzer, K.L., Reza Dana, M., and Sullivan, D.A. (2000). Impact of antiandrogen treatment on the fatty acid profile of neutral lipids in human meibomian gland secretions. *J. Clin. Endocrinol. Metab.* 85, 4866–4873. <https://doi.org/10.1210/jcem.85.12.7066>.
25. Krenzer, K.L., Dana, M.R., Ullman, M.D., Cermak, J.M., Tolls, D.B., Evans, J.E., and Sullivan, D.A. (2000). Effect of androgen deficiency on the human meibomian gland and ocular surface. *J. Clin. Endocrinol. Metab.* 85, 4874–4882. <https://doi.org/10.1210/jcem.85.12.7072>.
26. Wang, L.X., and Deng, Y.P. (2021). Androgen and meibomian gland dysfunction: from basic molecular biology to clinical applications. *Int. J. Ophthalmol.* 14, 915–922. <https://doi.org/10.18240/ijo.2021.06.18>.
27. Versura, P., Giannaccare, G., and Campos, E.C. (2015). Sex-steroid imbalance in females and dry eye. *Curr. Eye Res.* 40, 162–175. <https://doi.org/10.3109/02713683.2014.966847>.
28. Yoshida, M., and Apte, R.S. (2022). NAD(+) boosting brings tears to aging eyes. *Nat. Aging* 2, 97–99. <https://doi.org/10.1038/s43587-022-00172-5>.
29. Butovich, I.A. (2008). On the lipid composition of human meibum and tears: comparative analysis of nonpolar lipids. *Invest. Ophthalmol. Vis. Sci.* 49, 3779–3789. <https://doi.org/10.1167/iovs.08-1889>.
30. Chen, J., Green-Church, K.B., and Nichols, K.K. (2010). Shotgun lipidomic analysis of human meibomian gland secretions with electrospray ionization tandem mass spectrometry. *Invest. Ophthalmol. Vis. Sci.* 51, 6220–6231. <https://doi.org/10.1167/iovs.10-5687>.
31. Butovich, I.A., Borowiak, A.M., and Eule, J.C. (2011). Comparative HPLC-MS analysis of canine and human meibomian lipidomes: many similarities, a few differences. *Sci. Rep.* 1, 24. <https://doi.org/10.1038/srep00024>.
32. Lam, S.M., Tong, L., Yong, S.S., Li, B., Chaurasia, S.S., Shui, G., and Wenk, M.R. (2011). Meibum lipid composition in Asians with dry eye disease. *PLoS One* 6, e24339. <https://doi.org/10.1371/journal.pone.0024339>.
33. Chen, J., and Nichols, K.K. (2018). Comprehensive shotgun lipidomics of human meibomian gland secretions using MS/MS(all) with successive switching between acquisition polarity modes. *J. Lipid Res.* 59, 2223–2236. <https://doi.org/10.1194/jlr.D088138>.
34. Butovich, I.A., Suzuki, T., Wojtowicz, J., Bhat, N., and Yuksel, S. (2020). Comprehensive profiling of Asian and Caucasian meibomian gland secretions reveals similar lipidomic signatures regardless of ethnicity. *Sci. Rep.* 10, 14510. <https://doi.org/10.1038/s41598-020-71259-5>.
35. Suzuki, T., Kitazawa, K., Cho, Y., Yoshida, M., Okumura, T., Sato, A., and Kinoshita, S. (2022). Alteration in meibum lipid composition and subjective symptoms due to aging and meibomian gland dysfunction. *Ocul. Surf.* 26, 310–317. <https://doi.org/10.1016/j.jtos.2021.10.003>.
36. Penning, T.M., Burczynski, M.E., Jez, J.M., Hung, C.F., Lin, H.K., Ma, H., Moore, M., Palackal, N., and Ratnam, K. (2000). Human 3alpha-hydroxysteroid dehydrogenase isoforms (AKR1C1-AKR1C4) of the aldo-keto reductase superfamily: functional plasticity and tissue distribution reveals roles in the inactivation and formation of male and female sex hormones. *Biochem. J.* 351, 67–77. <https://doi.org/10.1042/0264-6021:3510067>.
37. Steckelbroeck, S., Jin, Y., Gopishetty, S., Oyesanmi, B., and Penning, T.M. (2004). Human cytosolic 3alpha-hydroxysteroid dehydrogenases of the aldo-keto reductase superfamily display significant 3beta-hydroxysteroid dehydrogenase activity: implications for steroid hormone metabolism

- p>and action.
- J. Biol. Chem.*
- 279, 10784–10795.
- <https://doi.org/10.1074/jbc.M313308200>
- .
38. Liu, S., Richards, S.M., Lo, K., Hatton, M., Fay, A., and Sullivan, D.A. (2011). Changes in gene expression in human meibomian gland dysfunction. *Invest. Ophthalmol. Vis. Sci.* 52, 2727–2740. <https://doi.org/10.1167/iops.10-6482>.
 39. Schroder, A., Abrar, D.B., Hampel, U., Schicht, M., Paulsen, F., and Garreis, F. (2016). In vitro effects of sex hormones in human meibomian gland epithelial cells. *Exp. Eye Res.* 151, 190–202. <https://doi.org/10.1016/j.exer.2016.08.009>.
 40. Simard, J., Ricketts, M.L., Gingras, S., Soucy, P., Feltus, F.A., and Melner, M.H. (2005). Molecular biology of the 3 β -hydroxysteroid dehydrogenase/delta5-delta4 isomerase gene family. *Endocr. Rev.* 26, 525–582. <https://doi.org/10.1210/er.2002-0050>.
 41. Hamada, Y., Sasaki, L., Uehara, H., Suzuki, T., Kinoshita, S., Otsuka, K., Kihara, A., Yamaguchi, Y., Miyake, T., and Doi, M. (2022). Optimising the method for visualising mouse meibomian gland using eyelid whole-mount lipid staining. *Ocul. Surf.* 26, 268–270. <https://doi.org/10.1016/j.jtos.2022.10.002>.
 42. Gibson, E.J., Stapleton, F., Wolffsohn, J.S., and Golebiowski, B. (2017). Local synthesis of sex hormones: are there consequences for the ocular surface and dry eye? *Br. J. Ophthalmol.* 101, 1596–1603. <https://doi.org/10.1136/bjophthalmol-2017-310610>.
 43. Simpson, E.R., and Davis, S.R. (2001). Minireview: aromatase and the regulation of estrogen biosynthesis—some new perspectives. *Endocrinology* 142, 4589–4594. <https://doi.org/10.1210/endo.142.11.8547>.
 44. Luu-The, V., and Labrie, F. (2010). The intracrine sex steroid biosynthesis pathways. *Prog. Brain Res.* 181, 177–192. [https://doi.org/10.1016/S0079-6123\(08\)81010-2](https://doi.org/10.1016/S0079-6123(08)81010-2).
 45. Labrie, F., Luu-The, V., Labrie, C., and Simard, J. (2001). DHEA and its transformation into androgens and estrogens in peripheral target tissues: intracrinology. *Front. Neuroendocrinol.* 22, 185–212. <https://doi.org/10.1006/frne.2001.0216>.
 46. Simard, J., Dumont, M., Soucy, P., and Labrie, F. (2002). Perspective: prostate cancer susceptibility genes. *Endocrinology* 143, 2029–2040. <https://doi.org/10.1210/endo.143.6.8890>.
 47. Olami, Y., Zajicek, G., Cogan, M., Gnessin, H., and Pe'er, J. (2001). Turn-over and migration of meibomian gland cells in rats' eyelids. *Ophthalmic Res.* 33, 170–175. <https://doi.org/10.1159/000055665>.
 48. Mantel, A., Carpenter-Mendini, A.B., Vanbuskirk, J.B., De Benedetto, A., Beck, L.A., and Pentland, A.P. (2012). Aldo-keto reductase 1C3 is expressed in differentiated human epidermis, affects keratinocyte differentiation, and is upregulated in atopic dermatitis. *J. Invest. Dermatol.* 132, 1103–1110. <https://doi.org/10.1038/jid.2011.412>.
 49. Inoue, T., Miki, Y., Kakuo, S., Hachiya, A., Kitahara, T., Aiba, S., Zouboulis, C.C., and Sasano, H. (2014). Expression of steroidogenic enzymes in human sebaceous glands. *J. Endocrinol.* 222, 301–312. <https://doi.org/10.1530/JOE-14-0323>.
 50. Suzuki, T., Nakata, T., Miki, Y., Kaneko, C., Moriya, T., Ishida, T., Akinaga, S., Hirakawa, H., Kimura, M., and Sasano, H. (2003). Estrogen sulfotransferase and steroid sulfatase in human breast carcinoma. *Cancer Res.* 63, 2762–2770.
 51. Levesque, E., Labriet, A., Hovington, H., Allain, E.P., Melo-Garcia, L., Rouleau, M., Brisson, H., Turcotte, V., Caron, P., Villeneuve, L., et al. (2020). Alternative promoters control UGT2B17-dependent androgen catabolism in prostate cancer and its influence on progression. *Br. J. Cancer* 122, 1068–1076. <https://doi.org/10.1038/s41416-020-0749-2>.
 52. Cermak, J.M., Krenzer, K.L., Sullivan, R.M., Dana, M.R., and Sullivan, D.A. (2003). Is complete androgen insensitivity syndrome associated with alterations in the meibomian gland and ocular surface? *Cornea* 22, 516–521. <https://doi.org/10.1097/00003226-200308000-00006>.
 53. Sullivan, D.A., Yamagami, H., Liu, M., Steagall, R.J., Schirra, F., Suzuki, T., Krenzer, K.L., Cermak, J.M., Sullivan, R.M., Richards, S.M., et al. (2002). Sex steroids, the meibomian gland and evaporative dry eye. *Adv. Exp. Med. Biol.* 506, 389–399. https://doi.org/10.1007/978-1-4615-0717-8_56.
 54. Safety and efficacy of testosterone 0.03% ophthalmic solution compared to vehicle for the treatment of MGD. (ClinicalTrials.gov Identifier: NCT00755183). <https://clinicaltrials.gov/study/NCT00755183?cond=NCT00755183&rank=1>.
 55. Geerling, G., Tauber, J., Baudouin, C., Goto, E., Matsumoto, Y., O'Brien, T., Rolando, M., Tsubota, K., and Nichols, K.K. (2011). The international workshop on meibomian gland dysfunction: report of the subcommittee on management and treatment of meibomian gland dysfunction. *Invest. Ophthalmol. Vis. Sci.* 52, 2050–2064. <https://doi.org/10.1167/iops.10-6997g>.
 56. Doi, M., Shimatani, H., Atobe, Y., Murai, I., Hayashi, H., Takahashi, Y., Fustin, J.M., Yamaguchi, Y., Kiyonari, H., Koike, N., et al. (2019). Non-coding cis-element of Period2 is essential for maintaining organismal circadian behaviour and body temperature rhythmicity. *Nat. Commun.* 10, 2563. <https://doi.org/10.1038/s41467-019-10532-2>.
 57. Doi, M., Takahashi, Y., Komatsu, R., Yamazaki, F., Yamada, H., Haraguchi, S., Emoto, N., Okuno, Y., Tsujimoto, G., Kanematsu, A., et al. (2010). Salt-sensitive hypertension in circadian clock-deficient Cry-null mice involves dysregulated adrenal Hsd3b6. *Nat. Med.* 16, 67–74. <https://doi.org/10.1038/nm.2061>.
 58. Butovich, I.A., and Suzuki, T. (2021). Effects of Aging on Human Meibum. *Invest. Ophthalmol. Vis. Sci.* 62, 23. <https://doi.org/10.1167/iops.62.12.23>.
 59. Star-Weinstock, M., Williamson, B.L., Dey, S., Pillai, S., and Purkayastha, S. (2012). LC-ESI-MS/MS analysis of testosterone at sub-picogram levels using a novel derivatization reagent. *Anal. Chem.* 84, 9310–9317. <https://doi.org/10.1021/ac302036r>.
 60. Doi, M., Satoh, F., Maekawa, T., Nakamura, Y., Fustin, J.M., Tainaka, M., Hotta, Y., Takahashi, Y., Morimoto, R., Takase, K., et al. (2014). Isoform-specific monoclonal antibodies against 3 β -hydroxysteroid dehydrogenase/isomerase family provide markers for subclassification of human primary aldosteronism. *J. Clin. Endocrinol. Metab.* 99, E257–E262. <https://doi.org/10.1210/jc.2013-3279>.
 61. Yamamura, K., Doi, M., Hayashi, H., Ota, T., Murai, I., Hotta, Y., Komatsu, R., and Okamura, H. (2014). Immunolocalization of murine type VI 3 β -hydroxysteroid dehydrogenase in the adrenal gland, testis, skin, and placenta. *Mol. Cell. Endocrinol.* 382, 131–138. <https://doi.org/10.1016/j.mce.2013.09.014>.

STAR★METHODS

KEY RESOURCES TABLE

REAGENT or RESOURCE	SOURCE	IDENTIFIER
Antibodies		
Rabbit monoclonal anti-AKR1C3/4	Abcam	Cat# ab209899, RRID:AB_2922995
Mouse monoclonal anti-HSD3B1	Abnova	Cat# H00003283-M01, RRID:AB_425493
Rabbit polyclonal anti-AKR1C4	Affinity Biosciences	Cat# DF9190, RRID:AB_2842386
Donkey anti-rabbit IgG, Alexa Fluor™ 594-conjugated	Thermo Fisher Scientific	Cat# A-21207, RRID:AB_141637
Donkey anti-mouse IgG, Alexa Fluor™ 488-conjugated	Cell Signaling	Cat# A-21202, RRID:AB_141607
Goat anti-rabbit IgG, peroxidase labeled polymer conjugated	Agilent	Cat# K4003, RRID:AB_2630375
Chemicals, peptides, and recombinant proteins		
Testosterone, [1,2,6,7- ³ H]	Perkin Elmer	Cat# NET370
5 α -dihydrotestosterone, [1,2,4,5,6,7- ³ H]	Perkin Elmer	Cat# NET926
Androst-4-ene-3,17-dione, [1 β - ³ H]	Perkin Elmer	Cat# NET453
Dutasteride	Cayman Chemical	Cat# 15956
Fadrozole hydrochloride	Sigma Aldrich	Cat# F3806
Testosterone, used in Figure 3	Tokyo Chemical Industry	Cat# T0027
Testosterone, used in Figure 4	FUJIFILM Wako Pure Chemical	Cat# 201-20551
Androstenedione	Tokyo Chemical Industry	Cat# A0845
Epiandrosterone	Tokyo Chemical Industry	Cat# E0374
Androstanedione, used in Figure 3	Matrix Scientific	Cat# 155569
Androstanedione, used in Figure 4	ALB Technology Limited	Cat# ALB-RS-04085
Androsterone, used in Figure 3	Cayman Chemical	Cat# 15872
Androsterone, used in Figure 4	FUJIFILM Wako Pure Chemical	Cat# 015-03971
5 α -androstane-3 α ,17 β -diol (3 α -diol)	Sigma Aldrich	Cat# A7755
5 α -androstane-3 β ,17 β -diol (3 β -diol)	Biosynth AG	Cat# FA17909
Testosterone-d3	Supelco	Cat# T2655
Epiandrosterone-d4	Cambridge Isotope Laboratories, Inc.	Cat# DLM-10269
Androstanedione-d4	ALSACHIM	Cat# C2125
Androsterone-d4	Cambridge Isotope Laboratories, Inc.	Cat# DLM-10402
Critical commercial assays		
Amplifex™ Keto Reagent	Sciex	Cat# 4465962
Dako REAL EnVision Detection System, Peroxidase/DAB, Rabbit/Mouse, HRP Kit	Agilent	Cat# K5007, RRID:AB_2888627
Software and algorithms		
Prism 8	GraphPad Prism	RRID:SCR_002798
LabSolutions	Shimadzu	RRID:SCR_018241
ProFSA Software	Perkin Elmer	Cat# ProFSA625TR

EXPERIMENTAL MODEL AND STUDY PARTICIPANT DETAILS

Animals

C57BL/6J male and female mice were purchased from Japan SLC and maintained on a 12-h light:12-h dark cycle with *ad libitum* access to food and water as described.⁵⁶ Mice were sacrificed by cervical dislocation for tissue collection at 3–4 months of age. All procedures were conducted in compliance with the Ethical Regulations of Kyoto University and performed under protocols approved by the Animal Care and Experimentation Committee of Kyoto University (Protocol #24-21).

Human participants

For this study, young, healthy Japanese participants aged 21–35 years were recruited from the local populations of Kyoto and Osaka, Japan, through a third-party corporation with no conflicts of interest. Participants confirmed the absence of systemic or ocular diseases via a written interview conducted prior to enrollment. Of the participants, 10 males and 10 females with no signs or symptoms of meibomian gland dysfunction (MGD) or dry eye disease (DE) were selected following an eye examination performed using a slit-lamp microscope. Participants self-reported their sex. The study, which involved clinical data collection and meibum sampling, received approval from the Institutional Review Board of Kyoto Prefectural University of Medicine (KPUM) [Protocol #ERB-C-2649]. All participants provided written informed consent and were enrolled in compliance with the principles of the Declaration of Helsinki. Exclusion criteria included anatomical or functional abnormalities of the eyelids, such as tumors; ocular allergies or infections; the use of punctal plugs or a history of surgical punctal occlusion; eye surgery within the past three months; contact lens use; anti-glaucoma treatments; or ongoing use of local or systemic antimicrobial or steroid medications. Meibum sampling and clinical data collection related to the meibomian glands and ocular surface were performed at Kyoto City Hospital (KCH).

Human eyelid specimens

Formalin-fixed, paraffin-embedded human eyelid samples obtained from postmortem donors of 41-year-old male and 34-year-old female, who had no history of eye-related diseases, both purchased from Science Care (Phoenix, Arizona, USA).

METHOD DETAILS

Testosterone radioactive tracing

The isolated upper eyelids (tarsal plates), testes or adrenal glands were incubated *in vitro* in pre-aerated Hank's balanced salt solution (HBSS) containing either 80 nM ³H-labelled Te (Testosterone, [1,2,6,7-³H]), DHT ([5 α -dihydrotestosterone, [1,2,4,5,6,7-³H]], or A4 (androst-4-ene-3,17-dione, [1 β -³H]) (all from PerkinElmer) for 3 h at 37°C with gentle vibration as described previously.^{14,57} Where indicated, 10 μ M dutasteride (Cayman Chemical) or fadrozole hydrochloride (Sigma) was included in medium. After incubation, steroids were extracted into 1 mL ethyl acetate from the tissues, followed by evaporation to dryness under nitrogen at 75°C with 2 μ L propylene glycol as a carrier solvent. The residues were dissolved using 43% acetonitrile (ACN) and filtered through a 0.22 μ m PVDF membrane. Samples were analyzed using a Waters e2695 high-performance liquid chromatography (HPLC) system coupled with an online flow scintillation analyzer (625TR series, PerkinElmer). Chromatographic separation was performed on a Lichrospher 100 RP-18 column (5 μ m, 250 \times 4 mm; Kanto Chemicals) with a LiChroCART guard column (5 μ m, 4 \times 4 mm; Merck) at 40°C. Gradient elution was performed using a mobile phase consisting of water (solvent A) and ACN (solvent B) at the flow rate of 0.7 mL/min and the following program: 43–46% B (0–30 min), 46–50% B (30–35 min), 50–100% B (35–40 min), 100% B (40–45 min), 100–43% B (45–50 min), and post run 10 min. Peak areas were quantified using the ProFSA software (PerkinElmer) and calculated as percentage of the sum of all peaks for each individual sample to compare data across samples. The RI chromatography in Figure 3A was performed using the same HPLC conditions as the LC-MS chromatography. The tissues boiled at 95°C for 5 min were used for negative control.

Testosterone tracing by LC-MS/MS

Non-radioactive testosterone was used for LC-MS/MS-based testosterone tracing. The tissues were incubated under the same conditions as those for radioactive tracing except increased concentration of testosterone (1 μ M) and elongation of incubation time (5 h) to allow sufficient quantification of all steroid metabolites by LC-MS/MS. The tissues boiled at 95°C for 5 min were used for negative control. Steroids were measured using a Shimadzu Nexera X2 Ultra HPLC system coupled to a triple quadrupole mass spectrometer (LCMS-8040, Shimadzu) with reference to authentic standards for adione (Matrix Scientific), ADT (Cayman Chemical), 3 β -diol (Biosynth AG) and 3 α -diol (Sigma-Aldrich), A4, Te and epiADT (all from Tokyo Chemical Industry). Chromatographic separation was performed on a Lichrospher 100 RP-18 column (5 μ m, 250 \times 4 mm; Kanto Chemicals) with a LiChroCART guard column (5 μ m, 4 \times 4 mm; Merck) at 40°C. Mobile phase consisted of water (A) and ACN (B), both containing 0.1% formic acid. Using a flow rate of 0.5 mL/min, chromatographic separation was achieved with the gradient elution time program as follows: 43–46% B (0–42 min), 46–50% B (42–49 min), 50–100% B (49–56 min), 100% B (56–63 min), 100–43% B (63–70 min), and 43% B (70–84 min). Metabolites were identified by comparing their retention times and the relative intensities of 3 multiple reaction monitoring (MRM) events with those of the authentic standards. The peak area of each metabolite target was analyzed using LabSolutions software (Shimadzu). The parameters for LC-MS/MS analysis in Figures 3 and S1 are shown in Table S2.

LC-MS/MS for human meibum profiling

Meibum was collected as described previously⁵⁸ and dissolved in 0.5 mL chloroform. Samples were stored in sealed glass tubes at –80°C before further processing. Quantitation of human meibum steroid was performed at Shimadzu Techno-Research (Kyoto, Japan). Unlabelled and deuterated standards were purchased from FUJIFILM Wako Pure Chemical Corporation (Te, ADT), Tokyo Chemical Industry (epiADT), ALB Technology Limited (adione), and Sigma-Aldrich Co. LLC (cholesterol). Testosterone metabolites were derivatized with a permanently charged quaternary aminoxy (QAO) reagent to enhance their ESI-MS/MS sensitivity.⁵⁹ For steroid quantification, 100 μ L of sample was spiked with 50 μ L internal standard (IS) mixture containing 2 ng/mL deuterated Te

(testosterone-d3, Supelco), epiADT (epiandrosterone-d4, Cambridge Isotope Laboratories, Inc.), adione (androstanedione-d4, ALSACHIM), and ADT (androsterone-d4, Cambridge Isotope Laboratories, Inc.) prior to evaporation to dryness in a centrifugal evaporator (CVE 3100). The residue was reconstituted in 10 μ L QAO reagent solution (Supelco-SigmaAldrich, Kyoto, Japan) and 40 μ L methanol containing 7%vol acetic acid. After 1 h of heating at 70°C, the samples were dried using a centrifugal evaporator (CVE 3100). Fifty microliters of water/methanol containing 7%vol acetic acid = 4:1 (v/v) solvent mixture was added and the samples were analyzed on a Shimadzu Nexera X2 Ultra HPLC system coupled to a triple quadrupole mass spectrometer (LCMS-8060, Shimadzu). For the quantification of total cholesterol, 5 μ L samples were spiked with 20 μ L IS solution containing 25 μ g/mL cholesterol-d7, 20 μ L methanol and 175 μ L KOH (0.35N). After heating at 50°C for 1 h, the samples were neutralized with 200 μ L methanol containing 5% acetic acid and filtered. The samples were analyzed on a UPLC-MS-MS system consisting of a Shimadzu Nexera X2 Ultra HPLC system (Shimadzu, Kyoto, Japan) and a 5500QTRAP mass spectrometer (Sciex, Framingham, MA, USA).

Testosterone metabolites derivatized with QAO reagent were analyzed using a Shim-pack Scepter C18-120 column (1.9 μ m, 2.1 mm I.D. \times 100 mm; Shimadzu, Kyoto, Japan). Mobile phase A was ultrapure water containing 0.1%vol formic acid and 2 mmol/L ammonium formate; mobile phase B was acetonitrile/water = 95/5 containing 0.1%vol formic acid and 2 mmol/L ammonium formate. The flow rate was set to 0.35 mL/min and the HPLC gradient was as follows: 0–0.75 min, 25% B; 0.75–13.0 min, 25–40% B; 13.0–14.0 min, 40–90% B; 14.0–17.0 min, 90% B; 17.0–17.1 min, 90–25% B; 17.1–20.0 min, 25% B. The MRM transitions and retention times for all compounds analyzed are shown in [Table S3](#).

Cholesterol was analyzed using a TSKgel column (5 μ m, 2.0 mm I.D. \times 50 mm; Tosoh, Japan). Mobile phase A was ultrapure water containing 0.1%vol formic acid; mobile phase B was acetonitrile containing 0.1%vol formic acid. The flow rate was set at 0.5 mL/min, and the HPLC gradient was as follows: 0.0–3.0 min, 90–100% B; 3.0–6.0 min, 100% B; 6.0–6.1 min, 100–90% B; 6.1–8.0 min, 90% B. The MRM transitions and retention times for all compounds analyzed are shown in [Table S3](#).

The linearity of the method was determined by analysis of standard plots associated with a freshly prepared seven-point standard calibration curve. Stock solutions of standards and internal standards were prepared in chloroform/methanol [2:1, (v/v)]. Calibration standard (CS) samples were prepared to give concentrations: 1.5, 7.5, 15, 75, 150, 750 and 1500 pg/mL for steroids and 4, 20, 40, 200, 400, 2000 and 4000 μ g/mL for cholesterol, while quality control (QC) samples were prepared with rabbit meibum at three concentrations: 15, 150 and 750 pg/mL for steroids and 40, 200 and 400 μ g/mL for cholesterol. The peak area ratios of analyte/IS compared to the nominal concentrations of each calibration standard point were plotted using a linear regression with a weighted factor of $1/x^2$ to calculate the concentration of each compound in the samples. The linear regression equation, correlation coefficient (r), linear range, and LOD are presented in [Table S4](#).

Immunohistochemistry and immunofluorescence staining

Five- μ m-thick eyelid paraffin sections were antigen-retrieved by pressure cooking in Tris-EDTA buffer (pH 9.0) as described¹⁴ and immersed into PBS containing 0.1% Tween 20 (PBS-T). Sections were blocked with 3% BSA in PBS-T for 2 h and incubated with a specific set of antibodies, including anti-AKR1C3+AKR1C4 antibody (rabbit monoclonal, EPR16726, Abcam, final concentration 0.4 μ g/mL for IHC and 0.7 μ g/mL for IF) and anti-HSD3B1 (mouse monoclonal, 3C11-D4, Abnova, final 0.05 μ g/mL for IHC and 0.5 μ g/mL for IF)⁶⁰ for 24 h at 4°C. The immunoreactivities were visualized with 3,3-diaminobenzidine using horseradish peroxidase-labeled anti-IgG polymers (Dako, EnVision+ System-HRP Labeled Polymer anti-rabbit for AKR1C3+AKR1C4 and anti-mouse for HSD3B1) or visualized using Alexa 594-conjugated anti-rabbit (for AKR1C3+AKR1C4) or anti-mouse (for HSD3B1) IgG (Thermo Fisher Scientific, 1:1000 dilution).⁶¹ For immunofluorescence, sections were mounted in medium containing 4',6-diamidino-2-phenylindole (DAPI) for counterstaining cell nuclei.

QUANTIFICATION AND STATISTICAL ANALYSIS

Statistical analysis was performed using GraphPad Prism 8. two-way ANOVA followed by Bonferroni's post-hoc tests were used to analyze statistical significance between groups. The results and details of statistics are available in corresponding figure legends and [Table S5](#). The results that reach statistical significance are indicated by * or # in the figures.